Macroscopic phase diagram and magnetocaloric study of metamagnetic transitions in the spin chain system $Ca_3Co_2O_6$

P. Lampen, N. S. Bingham, M. H. Phan,* and H. Srikanth*
Department of Physics, University of South Florida, Tampa, FL 33620, USA

H. T. Yi and S. W. Cheong
Rutgers Center for Emergent Materials and Department of Physics & Astronomy, Rutgers University, Piscataway, NJ 08854, USA
(Received 17 January 2014; revised manuscript received 26 March 2014; published 15 April 2014)

The magnetic entropy change (ΔS_M) in a single crystal of the geometrically frustrated spin chain system $Ca_3Co_2O_6$ has been determined under the influence of a wide range of temperatures and magnetic field variations. Our findings are consistent with the spin-density wave description of the zero field order, and with the suppression of the modulated state at low field. Metamagnetic transitions to the ferrimagnetic up-up-down configuration and full ferromagnetic alignment are observed upon the application of moderate magnetic fields in the *c* direction. At low temperatures, an increase in ΔS_M supports the presence of short-range magnetic correlations coexisting with long-range order up to large fields. Depending on the temperature regime, local maxima or minima in $\Delta S_M(H)$ can be found within the ferrimagnetic phase, which are identified with intermediate configurations among the chains. A new magnetic phase diagram has been constructed from the magnetic field and temperature dependence of magnetic entropy change.

DOI: 10.1103/PhysRevB.89.144414 PACS number(s): 75.47.Lx, 75.30.Sg

I. INTRODUCTION

The magnetic behavior of the spin chain cobaltite $Ca_3Co_2O_6$ combines geometric frustration with intrinsic low dimensionality, giving rise to complex physical phenomena that continue to attract a great deal of interest [1–7]. Crystallizing in the rhombohedral space group $R\bar{3}c$ [8], $Ca_3Co_2O_6$ consists of face-sharing CoO_6 trigonal prisms and CoO_6 octahedra alternating along the *c* axis to form chains. As a result, the system exhibits pronounced quasi-one-dimensional magnetic characteristics. With six nearest neighbors, the CoO_6 chains form a triangular lattice in the *ab* plane, separated by nonmagnetic Ca atoms (Fig. 1). Due to the nature of its geometry and single-ion axial anisotropy, $Ca_3Co_2O_6$ has long been considered to be a model triangular-lattice Ising antiferromagnet, where each chain can be represented by a single rigid spin on a two-dimensional (2D) lattice [9]. However, more recent theoretical predictions and experimental results have shown this description to be oversimplified, and a full three-dimensional (3D) picture must be invoked to account for the wide range of unusual physical phenomena found in the system [1,5,10]. Intrachain Co-Co separation is approximately one half of the interchain Co-Co distance, contributing to large anisotropy and competing exchange interactions: ferromagnetic (FM) coupling along the chains (J_1) and weak antiferromagnetic (AFM) coupling between nearest- and next-nearest-neighbor chains through a helical Co-O-O-Co super-superexchange pathway (J_2, J_3) [2,10–12], leading to significant magnetic frustration.

Neutron diffraction, magnetization, and specific heat studies [13–15] indicate long-range magnetic ordering below $T \sim 25$ K, in good agreement with the predicted strength of the intrachain FM exchange parameter ($J_1 \sim 25$ K) [2]. The ordered state in zero field is similar to the partially disordered antiferromagnetic (PDA) phase found in some geometrically frustrated ABX_3 compounds such as $CsCoCl_3$ and $RbFeB_3$, in which ⅔ of the chains couple antiferromagnetically, with the remaining ⅓ incoherent (no long-range order along the chain; no coupling with neighboring chains) [15–18]. However, resonant x-ray scattering [19] revealed incommensurate magnetic order along the chains, implying a long wavelength spin-density wave (SDW). Subsequent neutron scattering and computational results have unambiguously established the existence of a SDW along the *c* axis with long periodicity (up to ~1000 Å), with a phase shift of 120° between adjacent chains [1,10,12,14]. As a consequence of the amplitude modulation of the intrachain moment, the up-down-incoherent triangular unit of the PDA phase is only realized at specific points along the *c* axis.

The application of a small magnetic field on a triangular Ising-like AFM lattice has the effect of lifting degeneracy and imparting a preferred orientation to the incoherent spin chain, resulting in a ferrimagnetic up-up-down configuration among the chains with a magnetization equal to ⅓ of the saturation value (M_S) [20]. Indeed, a magnetization plateau with $M \sim M_S/3$ is a well-known feature of $Ca_3Co_2O_6$ below the critical magnetic field (~3.6 T) where FM order is established [6,15]. The more unique aspects of the field-driven magnetization curves occur below 10 K, where additional plateaus emerge in the magnetization at regular field intervals (1.2 T, 2.4 T, 3.6 T, with higher field steps occasionally observed), accompanied by an increase in magnetic hysteresis. Due to similarities with experimental results on single-molecule magnets, quantum tunneling of magnetization (QTM) was proposed as the driving mechanism behind the multiple step behavior [21]; however, this idea has been challenged [22,23]. The appearance of the additional plateaus corresponds to the onset of extremely slow spin dynamics, while their number and height depend strongly on history and sweep rate, indicating

*Corresponding authors: phanm@usf.edu and sharihar@usf.edu

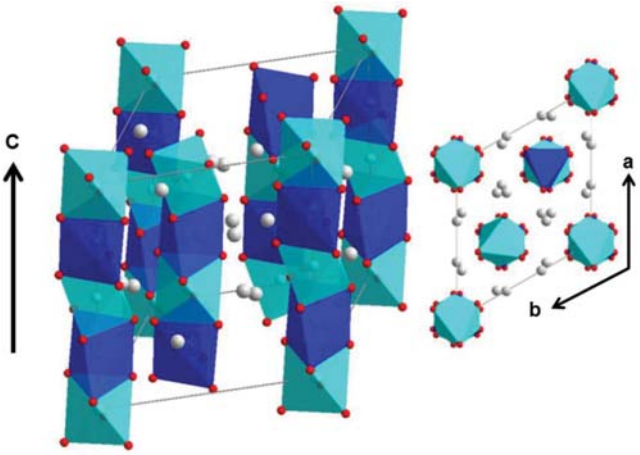

FIG. 1. (Color online) Representation of $Ca_3Co_2O_6$ crystal structure from Ref. [23]: stacked Ca/O octahedra (light blue) and trigonal prismatic (dark blue) polyhedral chains run along the *c* axis. Oxygen atoms are shown in red. Right: the chains form a triangular lattice in the *ab* plane separated by Ca atoms (gray).

that nonequilibrium processes underlie this phenomenon [1,4,20,24–26].

Although the question of the true ground state of this complex frustrated spin chain system and its temperature and time variation have been highly scrutinized, less work has been undertaken on the field dependence of the magnetic order at intermediate temperatures. Several phase diagrams can be found in the literature based on bulk magnetization [15,27,28] and muon spin relaxation measurements [29]. However, these do not take into account the current understanding of the SDW ground state or the more recently described low-temperature short-range order phase [5,7,23]. In this work we have applied the magnetic field and temperature dependence of magnetic entropy change as a probe of the magnetic states of $Ca_3Co_2O_6$. The results obtained are fully consistent with recent findings [5,7], thus allowing us to establish a more comprehensive magnetic phase diagram for this exotic system.

The magnetic entropy change (ΔS_M) in a system is related to the magnetic field (H) and magnetization (M) through the thermodynamic Maxwell relation, which yields an expression for the isothermal ΔS_M produced by a magnetic field change of $\Delta H = H_f - H_i$ [30]:

$$\Delta S_M(T) = \mu_0 \int_{H_i}^{H_f} \left(\frac{\partial M(T,H)}{\partial T} \right)_H dH. \qquad (1)$$

It follows that $\Delta S_M(T)$ reaches its maximum value where the derivative $\partial M/\partial T$ is largest, resulting in a peak in the entropy change where the magnetization changes rapidly near a phase transition. In addition to its conventional use in characterizing materials for magnetic refrigeration applications, we have recently demonstrated that the magnetic entropy change also provides a useful tool to study phase transitions and magnetic states subject to an applied field [31–35]. The sensitivity of the magnetic entropy change to small changes in the magnetization, given its relation to $\partial M/\partial T$ combined with the dependence of the sign of $\Delta S_M(T)$ on the macroscopic spin configuration of a magnetic system, make the study of unusual phase transitions and phase coexistence in strongly correlated systems possible through careful analysis of the evolution of ΔS_M with temperature and applied field.

II. EXPERIMENT

High-quality single-crystalline samples of $Ca_3Co_2O_6$ were grown using a flux technique with K_2CO_3 and KCl flux [27]. This method yielded needlelike single crystals with dimensions up to 7 × 1.5 × 1.5 mm. Measurements of the temperature dependence of magnetization and the magnetic entropy change associated with the magnetocaloric effect were performed in a commercial Physical Property Measurement System (PPMS) from Quantum Design with a vibrating sample magnetometer (VSM) attachment. Isothermal magnetization curves were collected over a temperature range of 2–20 K at intervals of 1 K, and 10–120 K at intervals of 5 K. The magnetic field was stabilized before taking a data point every 0.07 T with a sweep rate of 0.01 T/s between points up to a maximum field of 7 T. In the low-temperature region (2–20 K), the system was warmed to 100 K—well above the onset of long-range magnetic order—in between the acquisition of each $M(H)$ curve in order to clear the sample history and minimize the development of time-dependent phases. Using the AC/DC Magnetometry System (ACMS) option of the PPMS, both the real $\chi'(T)$ and imaginary $\chi''(T)$ components of the ac susceptibility were simultaneously measured while warming up from 5 K. In all cases, the external field was directed along the *c* axis of the crystal.

III. RESULTS

Figure 2 shows the characterization of the magnetization along the easy direction of the single crystal under the field-cooled cooling (FCC), field-cooled warming (FCW), and zero-field-cooled warming (ZFC) protocols. The expected

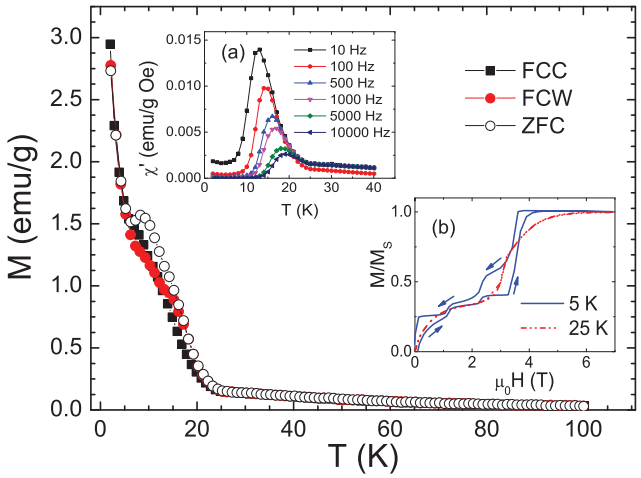

FIG. 2. (Color online) Temperature-dependent magnetization curves collected under the ZFC, FCC, and FCW protocols under an applied dc field of 10 mT. Inset (a): Temperature-dependent ac susceptibility taken at an ac field of 0.1 mT for varying frequencies. Inset (b): Magnetic-field-dependent magnetization curves at 25 and 5 K.

sharp growth of magnetization is observed in the $M(T)$ curves below 25 K as the onset of long-range magnetic order in the intrinsically frustrated system leads to a large increase in susceptibility. A splitting between the magnetization curves measured while warming up and cooling down for $T < 25$ K shows that thermal hysteresis is present throughout the ordered temperature region. At 25 K, two steps are observed in the $M(H)$ curves [Fig. 2(b)] with plateaus at $M \sim M_S/3$ from small fields (corresponding to ⅔ of the chains aligned with the field and ⅓ of the chains antialigned), and $M \sim M_S = 4.8\,\mu_B$/f.u. for $H \geq 3.3$ T; this second critical field approaches 3.6 T as the temperature decreases. For $T = 5$ K, two additional steps are observed to split the first magnetization plateau at 1.2 T and 2.4 T, although the number of steps—corresponding to switching between metastable states—can vary according to the sweep rate.

Bifurcation of the magnetization curves collected under ZFC and FCW protocols occurs at ~18 K, and a cusp in the ZFC curve marks the crossover in relaxation mechanisms below ~8 K [36]. A shift in the peak location of the ac susceptibility curves with varying frequency further demonstrates the slow dynamics of the geometrically frustrated system [Fig. 2(a)]. The peak shift is characterized by the phenomenological parameter often used to compare spin glass systems, $K = \Delta T_f/(T_f \Delta \log f)$, where T_f is the freezing temperature taken as the peak in $\chi''(T)$. The value of $K = 0.171$ calculated from our susceptibility data, in good agreement with the results of Maignan *et al*. [27], is outside the expected range for conventional spin glasses (0.005–0.01) [37] and superparamagnetic compounds (0.10–0.13) [38]. However, the related compounds Ca_3CoIrO_6 [39] and Ca_3CoRhO_6 [40] show frequency dependence in the superparamagnetic range, emphasizing the unique aspects of $Ca_3Co_2O_6$ even among other spin chain systems.

The magnetic entropy change in the system is calculated through the application of Eq. (1) to a series of $M(H)$ isotherms collected across the temperature region of interest in $Ca_3Co_2O_6$. The temperature and field dependence of the entropy change ($\Delta S_M(T, H)$) is shown in Fig. 3. The dominant feature in $\Delta S_M(T)$ is a minimum near the long-range ordering temperature 25 K [Fig. 3(a)]; however, finite negative values of ΔS_M persist up to 120 K, signifying weak FM interactions at high temperatures. In general, a decrease in ΔS_M upon the application of an external magnetic field is associated with FM alignment in a material as the Zeeman energy suppresses thermal fluctuations, thus reducing the entropy of the spin system. On the other hand, an increase in magnetic entropy with field in an antiferromagnet can be observed as moderate applied fields may decouple individual spins from sublattices aligned in opposition to the applied field direction [41,42]. The development of FM correlations within the chains well above 25 K would account for the gradual high-temperature fall off the magnetization (Fig. 2) and entropy change [Fig. 3(a)]. Such short-range magnetic interactions within the chains are also suggested by anomalies in extended x-ray absorption fine structure (EXAFS) [11], Mössbauer [43], and magnetoelectric results [3] in this temperature range.

Below 25 K, more complex temperature- and field-induced features are apparent in the $\Delta S_M(H,T)$ surface [Fig. 3(b)], indicating that several types of magnetic order are present. The details of the local features in the entropy change are best understood through an examination of its field dependence at several representative temperatures. The gradual and uniform decrease in $\Delta S_M(H)$ at $T = 30$ K [Fig. 4(a)] with increasing external field strength is a signature of the short-range correlations discussed above, as localized FM clusters in the chains are stabilized and expanded by the application of a moderate field. As the temperature is decreased below the onset of long-range order, the variation of ΔS_M with applied field becomes nontrivial. At 15 K, ΔS_M exhibits a minimum at $H_{C1} \sim 2$ T [Fig. 4(b)] and then increases in the range 2 T $< H <$ 3.5 T. As established from Fig. 2 and previous reports [6,15,23], by 2 T the compound is in the ferrimagnetic (FIM) up-up-down configuration. A second metamagnetic transition

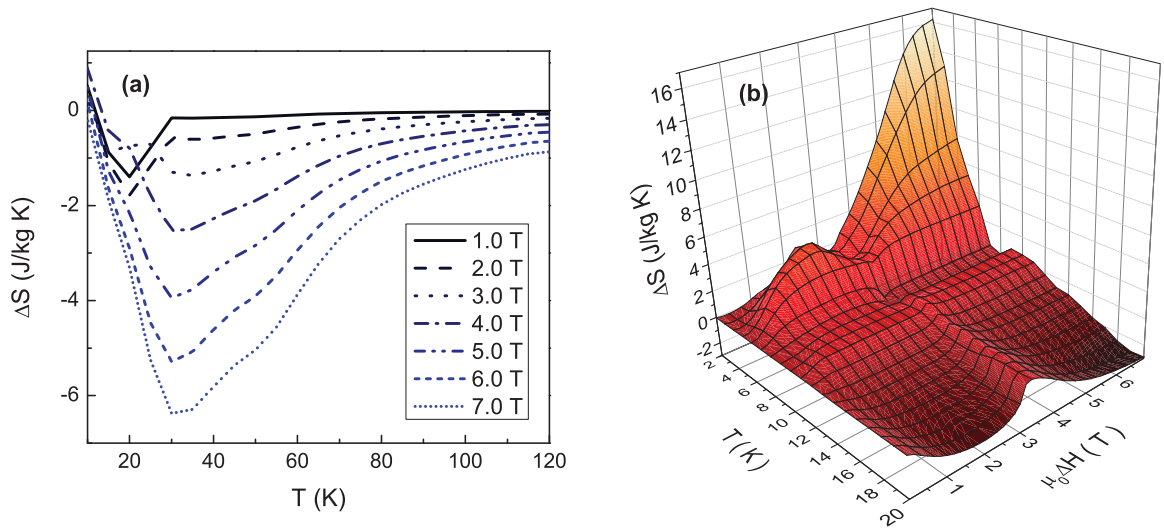

FIG. 3. (Color online) Change in magnetic entropy as a function of temperature and applied magnetic field, calculated via the thermodynamic Maxwell relation for (a) 10 K $\leq T \leq$ 120 K with 5 K temperature interval and 1 T field interval and (b) 2 K $\leq T \leq$ 20 K with 1 K temperature interval and 0.07 T field interval.

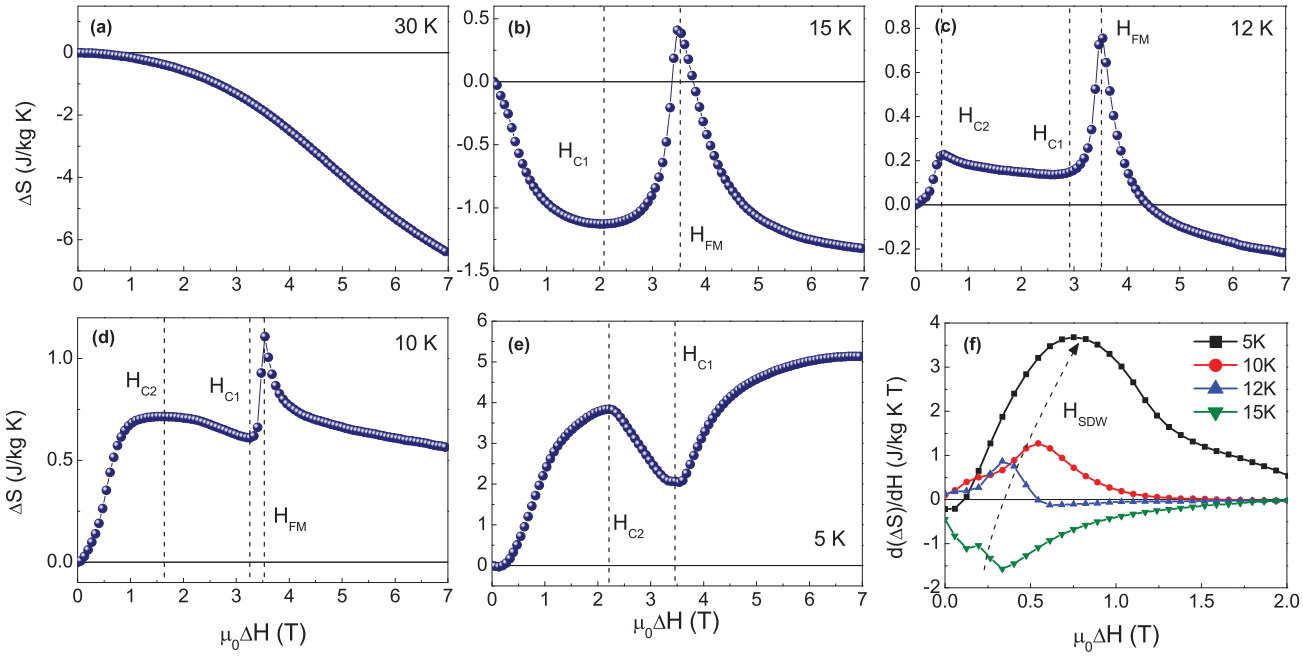

FIG. 4. (Color online) Magnetic entropy change as a function of applied magnetic field at various constant temperatures, (a) 30 K, (b) 15 K, (c) 12 K, (d) 10 K, and (e) 5 K. (f) First derivative of magnetic entropy change with applied field.

to FM order is induced at $H_{FM} \sim 3.5$ T, above which $\Delta S_M(H)$ decreases monotonically with applied field as expected in a FM material. The minimum value in the entropy $\Delta S_M(H_{C1})$ increases as the temperature is lowered, with a crossover in the initial (low field) entropy change from negative to positive at 12 K [Fig. 4(c)]. The entropy change below 12 K is characterized by the emergence of a positive peak at a field H_{C2} that increases as the temperature is lowered and reaches ~2.4 T at 2 K. The field required to saturate the sample also increases rapidly below 12 K, such that by 5 K, no critical field exists above which the entropy change decreases uniformly, i.e., a homogeneous FM phase is not established up to 7 T.

At low temperature, $Ca_3Co_2O_6$ is characterized by very slow dynamics and a unique time-dependent order-order transition [5,21]. Therefore, the measurement protocol, in particular thermal history, is an important consideration in evaluating the observed magnetization and hence the magnetic entropy change. To illustrate these effects, $\Delta S_M(T, H)$ was calculated after acquiring a second set of data between 20 and 2 K without the intermediate warming step, i.e., measuring an M (H) isotherm, decreasing the temperature by 1 K, then acquiring the next isotherm immediately after temperature stabilization, for an effective cooling rate of ~1.2 K h^{-1}. Figure 5 compares the entropy change as a function of temperature for measurement protocols with (solid symbols) and without (open symbols) the intermediate warming step. In the data collected without warming, ΔS_M reaches very large apparent values of close to 40 J/kg K at base temperature subject to an applied field of 7 T.

IV. DISCUSSION

Distinct relaxation mechanisms have been observed at very low and higher temperatures in $Ca_3Co_2O_6$, with an intermediate regime over which the two relaxation processes have a comparable effect [21]. Above 14 K, the $\Delta S_M(T)$ curves at a given field in Fig. 5 lie on top of one another. However, at the onset of the slowing dynamics, there is a splitting between the data obtained under different protocols. The temperature of the divergence of $\Delta S_M(T)$ is in good agreement with the appearance of short-range magnetic order, as discussed below. It is well known that a changing magnetic field applied in

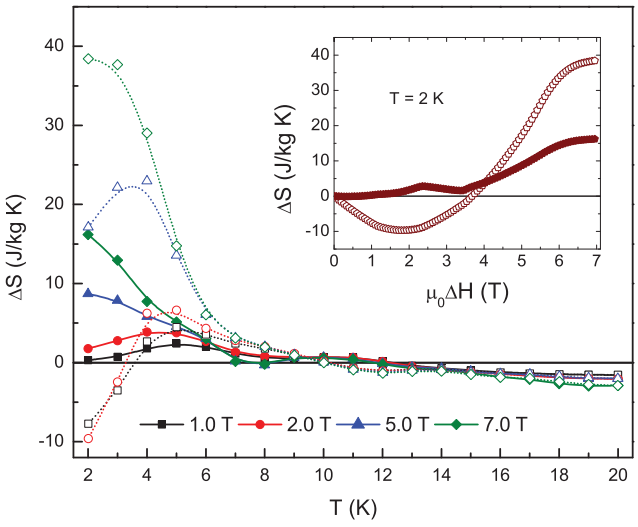

FIG. 5. (Color online) Comparison of magnetic entropy change as a function of temperature for measurement protocols with and without warming between isotherms (solid symbols and open symbols, respectively). Inset: Field dependence of the entropy change at 2 K.

a glassy region introduces nonequilibrium and aftereffects, and for this reason the use of the Maxwell relation is strictly valid only when the system is in thermodynamic equilibrium [44,45]. Similar nonequilibrium effects occur in the course of a first-order transition, and thus the magnetization results depend on the kinetics of the transition and therefore the experimental procedure [45]. It has been shown that artifacts associated with the use of the Maxwell relation at a first-order transition can be eliminated by warming the sample well above T_C, ensuring that the transition is always crossed in the same manner [46]. We take a similar approach in measuring $\Delta S_M(T)$ for analysis. It can be seen (Fig. 4) that more extreme apparent values of magnetic entropy change occur when the warming step is not undertaken. In this case, remanent effects from repeated application and removal of a field in the low-temperature region with extremely slow dynamics result in arbitrarily large differences in the magnetic state between successive isotherms.

In addition to standard glassy effects, a small amount of a time-dependent commensurate antiferromagnetic (CAFM) phase may be present in the system for the data taken without warming, since the thermal history is not erased. An ultraslow zero-field order-order transition between the incommensurate SDW and the commensurate CAFM phase with distinct translational symmetry occurs between ~8 and 12 K [5,12,47]. The CAFM phase evolves with a characteristic time $\tau = 1.4$ h at 10 K and $\tau = 3.9$ h at 8 K, and the transition is never complete [5]. In the sample rapidly cooled (~2 K/min) to 2 K, the magnetic state is "frozen in," and the CAFM phase is not present. Even when held at higher temperatures (8–12 K) where the dynamics are such that the transition may occur, a detailed study of the time dependence of the relative phase fractions found no significant signature of the CAFM phase after the first 15 min [5]. Therefore, the presence of the CAFM phase can be excluded in the case of the magnetization data collected under the warming protocol (Fig. 3) in which the system was cooled rapidly (in excess of 2 K/min) to each temperature of interest, and a magnetic field was applied to initiate the M (H) measurement immediately after temperature stabilization.

In the earliest proposed phase diagram for $Ca_3Co_2O_6$ by Kageyma *et al*. [15] [Fig. 6(a)], as well as the later works of Maignan *et al*. [27] and Goko *et al*. [28], the establishment of the FIM state in the high-temperature region was shown to occur only after the application of a substantial magnetic field. In these cases, the critical field was taken as the field at which the magnetization of the M (H) curve crosses $M_S/3$. Determined in this way, the apparent crossover field from the zero-field state to the FIM state will be quite large due to significant rounding of the steps just below 25 K. However, the majority of the growth in magnetization in the initial field-induced step occurs almost immediately when a field is introduced. Indeed, calculations have shown that a weak field breaks the ground state degeneracy, resulting in the FIM up-up-down phase, while rounding of the steps could be accounted for by a random exchange term simulating the inhomogeneity of a real system [25] The AFM and FM Bragg peaks that collectively describe the FIM phase also showed a rapid step close to 0 T [7,47]. Thus the overall magnetic order is up-up-down from very small fields, although the spin

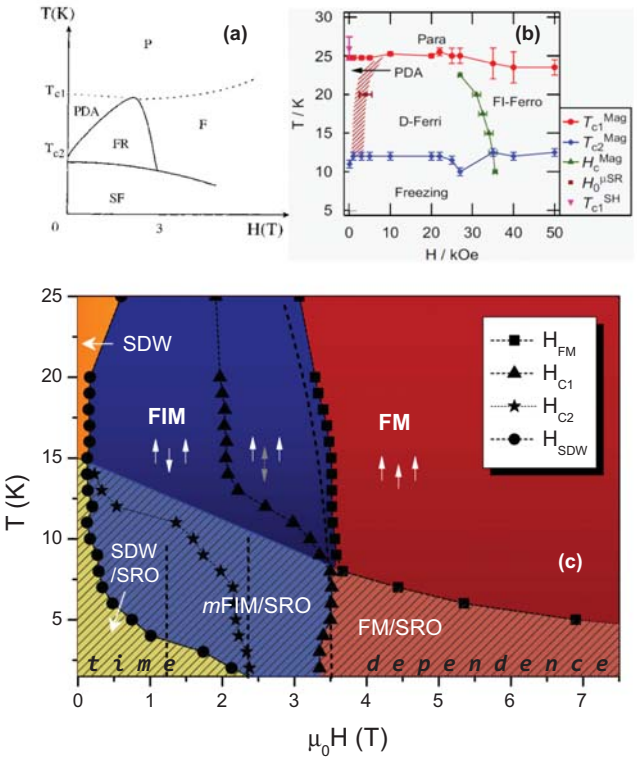

FIG. 6. (Color online) (a) Phase diagram proposed by Kageyama *et al*. (Ref. [15], reproduced with permission). (b) Phase diagram proposed by Takeshita *et al*. (Ref. [29], reproduced with permission). (c) Magnetic phase diagram including ferromagnetic (FM), ferrimagnetic (FIM), metastable FIM (*m*FIM), short-range-order (SRO), and spin-density wave (SDW) phases derived from critical points of the field- and temperature-dependent magnetic entropy change as described in the text. Dashed lines represent locations of the magnetization steps taken from M (H) curves.

chains cannot be described as perfectly rigid due to thermal fluctuations. In Fig. 4(b), the negative values of magnetic entropy change observed for $H < H_{C1}$ are consistent with enhanced intrachain FM order (reducing the configurational entropy) resulting from an increase in the axial applied field. Therefore, given the known relationship among chains on the triangular lattice unit at the end points of field range $H_{C1}(\uparrow\uparrow\downarrow) < H < H_{FM}(\uparrow\uparrow\uparrow)$, it is reasonable to attribute the increase in the entropy across this interval to the reversal of the third chain. This process is quite extended in field; however, we note that it involves the flipping of a large (theoretically infinite) number of individual spins against the satisfied FM interchain interaction at a high cost in energy.

As the temperature is lowered, a crossover occurs from a decrease in ΔS_M with field to a strong initial increase—pointing to growing disorder in the system. An unusual drop in the intensity of AFM reflections at low temperature has been noted in $Ca_3Co_2O_6$ by several groups [48,49]. This phenomenon has been attributed to the existence of short-range magnetic ordering with a correlation length ~180–250 Å coexisting with long-range order phases at zero field [7,14], and resonant x-ray scattering has confirmed that only a fraction of the total spin moments contribute to the signal in the SDW

state, with the rest exhibiting short-range order (SRO) [23]. Such SRO is manifested as a Lorentzian contribution to the AFM Bragg peaks that appears below 15 K, and reaches a maximum at 8 K with an equilibrium volume fraction of ~0.4 [5,7]. While some description of the properties of the SRO phase has been provided experimentally, such methods are not suited to address its origin. However, theoretical investigations of the magnetization steps have shown domains of reduced metastable magnetization that may be related to the observations of SRO: In several studies, authors defined cells of spin chains with various discrete energies (e.g., ranging from −6 to +6) depending on the number of "up" (+1) and "down" (−1) nearest neighbors [4,22,26,27]. In a small applied field, while cells corresponding to the up-up-down configuration formed the majority phase, significant numbers of cells with different energies were also present. These differently configured spin chain units tended to chain or cluster into interlinked domains [4,22,26].

From Fig. 4(c)–4(e), the presence of the SRO AFM phase, expected to contribute to the total magnetic entropy in a positive manner, is evident from the observation of $\Delta S_M > 0$ for all applied fields at low temperatures. A positive peak in ΔS_M ($H = H_{C2}$) is the predominant feature in the low- to moderate-field range below ~10 K. While the origin of the peak is unclear, given its observed temperature dependence it is most likely associated with the presence of SRO. For 10 K $< T <$ 15 K, the SRO phase is present but not significant, based on the small values of H_{C2} and ΔS_M (H_{C2}). As $T \to 2$ K, H_{C2} approaches 2.4 T, the field at which the second fractional magnetization plateau is seen in the M (H) curves. Recent Monte Carlo results predict a fractional reversal of spin chains as the magnetic field is increased just below the second magnetization step, which initially introduces more disorder into chains aligned against the field [26]. This may be related to our observation of a local maximum in $\Delta S_M(H)$ near this field at base temperature; however, we note that the exchange constant J_3 was neglected in this model. It is clear from the monotonic increase of ΔS_M and the nonsaturation of the magnetization below 6 K that some degree of the SRO phase persists up to the highest fields available in our experimental setup. Indeed, it was observed that at 2 K, the short-range contribution to the neutron diffraction patterns decreased in a stepwise fashion at fields corresponding to the magnetization plateaus but retained nonzero intensity even above 3.6 T [7]. Our current results and other reports [1,4,23] indicate that the overall magnetic order for $H < H_{C1}$ is ferrimagnetic at low temperatures, although with greater complexity than the up-up-down configuration established for $T >$ 10 K. Collectively, the intermediate chain configurations in the multiple-magnetization-step range can be described as belonging to a metastable ferrimagnetic (mFIM) phase.

Spin-density wave ground states are not uncommon in geometrically frustrated triangular lattice antiferromagnets, which possess strong single-ion anisotropy, but are generally sensitive to perturbations such as a magnetic field [50]. In $Ca_3Co_2O_6$, the field-induced transformation from the zero-field SDW to the FIM phase must necessarily be complete once sufficient field is applied to result in the initial magnetization step, where the FIM phase is unambiguously established. In the $\Delta S_M(H)$ curves measured between 2 and 25 K, we note the absence of a clear feature (i.e., a peak) in an appropriate field range to be attributed to the suppression of the SDW. However, a change in slope at low fields, visible as a peak in a plot of $d(\Delta S_M)/dH$ vs H (Fig. 4(f)), points to a shift in the balance of phases contributing to the magnetic entropy. The field-induced crossover from the SDW to the FIM phase was observed directly by Mazzoli *et al.* [23] with resonant magnetic x-ray scattering (RMXS) as an incommensurate to commensurate "lock-in" transition. At 5 K, this transition occurred at ~0.4 T, in good agreement with the peak location we find in $d(\Delta S_M)/dH$. Crossover fields reported for various temperatures in Ref. [47] show similarly good agreement with the low-field slope change in ΔS_M, providing additional support for the interpretation of this feature as the relaxation of the SDW, hereafter referred to as H_{SDW}. This critical field is more or less temperature independent between 20 and 10 K (~0.1–0.2 T), but it grows significantly at low temperatures. In order to exit the SDW phase, the system must decrease the coherence length of the chains in the c direction in order to minimize the energy required to relax the modulation, which has a periodicity of up to 1000 Å in $Ca_3Co_2O_6$ [10,23]. The frozen free-energy landscape at very low temperatures in this frustrated system makes such a relaxation increasingly costly in terms of Zeeman energy.

In Fig. 6(c), a phase diagram is constructed based on our observations of the magnetic entropy change in $Ca_3Co_2O_6$. The field at which the system enters the FM state (H_{FM}) is taken as the field above which ΔS_M decreases uniformly. This value remains close to 3.6 T for all temperatures below 25 K, in agreement with the location of the step in magnetization, marked by a dashed line. Between H_{C1} and H_{FM}, the entropy of the system increases during the flipping process of the third spin chain in the up-up-down configuration. Short-range correlations with an AFM character are present below 15 K and grow in volume fraction as the temperature is lowered, resulting in a crossover from $\Delta S_M(H) < 0$ to $\Delta S_M(H) > 0$ at 12 K. The SRO phase is affected by magnetic fields, but below 6 K, it is not completely suppressed up to 7 T. A line bordering the region in which the SRO phase contributes significantly to the magnetic behavior is extrapolated between the point at which H_{FM} begins to increase and the emergence of H_{C2}—a local maximum in $\Delta S_M(H)$ due to field-induced disorder in chains aligned in opposition to the applied field. Below ~12 K, slowing dynamics result in the dependence of the observed features on measurement protocol. Figure 6(c) thus presents the "rapid-cooled" phase diagram of $Ca_3Co_2O_6$; modifications can be expected at low temperatures if the CAFM phase is allowed to develop or the thermal history is not erased between successive measurements.

The first proposed phase diagram for $Ca_3Co_2O_6$ by Kageyama *et al.* in 1997 [15] [Fig. 6(a)] relied on the steps in the M (H) curves to define the boundaries between FIM and FM phases and predicted a PDA order at zero field. A nearly identical magnetization-derived diagram was reported in 2004 [28] and modified in 2007 via muon spin relaxation (μSR) [Fig. 6(b)] by Takeshita *et al.* [29]. As discussed above, the boundary between the zero-field order (identified in all cases as PDA) was taken as the point at which $M = M_S/3$ by Kageyama *et al.* [15] and Goko *et al.* [28], resulting in large

critical fields. It is interesting to note that in Fig. 6(b), the μSR data at 20 K indicate a change in slope of the relaxation time at 0.4 T, attributed by the authors to the boundary between the PDA and FIM phases [29]. Given the good agreement, it is likely that this field corresponds to the suppression of the SDW subsequently observed by Mazzoli *et al*. [23] and in the current magnetic entropy study. In all previous phase diagrams, the appearance of irreversibility in the ZFC and field-cooling M (T) curves at ∼10–12 K was taken to indicate the spin freezing temperature, below which the PDA phase was no longer present and no features were reported, in contrast to more recent observations showing that the long-range zero field order (SDW rather than PDA) persists to 2 K [5]. The utilization of the temperature- and field-dependent ΔS_M results has allowed us to modify the phase diagram to reflect the current understanding of the role of SDW and SRO phases in $Ca_3Co_2O_6$, as well as to extend results to temperatures below the onset of slow dynamics (∼10 K). Although derived from bulk magnetization, the magnetic entropy calculations provide greater sensitivity to field-induced variation within macroscopic phases. This has allowed us to resolve subfeatures of the FIM phase, including the field extent of conversion between the up-up-down and up-up-up configurations at high temperature that has not previously been reported, as well as a critical field H_{C2} at which a maximum entropy occurs in the *m*FIM region. These phenomena are of interest for further study with more direct experimental probes (e.g., neutron and/or x-ray scattering) and computational techniques.

V. CONCLUSIONS

The phase diagram of the frustrated spin chain compound $Ca_3Co_2O_6$ was established over a wide range of fields and temperatures by an investigation of the magnetic entropy change in the system. The present results are consistent with the SDW description of the ground state at zero field and indicate the suppression of the modulated state in favor of a FIM up-up-down arrangement of the spin chains with the application of a moderate field. Below 15 K, a high degree of disorder induced by low magnetic fields points to a significant contribution from a phase with short-range order.

ACKNOWLEDGMENTS

Research at the University of South Florida was supported by the U.S. Department of Energy, Office of Basic Energy Sciences, Division of Materials Sciences and Engineering under Award No. DE-FG02-07ER46438 (magnetic studies). The work at Rutgers University was supported by the DOE under Grant No. DE-FG02-07ER46382 (synthesis of samples).

[1] Y. Kamiya and C. D. Batista, Phys. Rev. Lett. **109**, 067204 (2012).
[2] G. Allodi, P. Santini, S. Carretta, S. Agrestini, C. Mazzoli, A. Bombardi, M. R. Lees, and R. De Renzi, Phys. Rev. B **89**, 104401 (2014).
[3] T. Basu, K. K. Iyer, K. Singh, and E. V. Sampathkumaran, Sci. Rep. **3**, 3104 (2013).
[4] Y. Hu, G. Z. Wu, Y. Liu, X. L. Yang, and A. Du, J. Magn. Magn. Mater. **337**, 46 (2013).
[5] S. Agrestini, C. L. Fleck, L. C. Chapon, C. Mazzoli, A. Bombardi, M. R. Lees, and O. A. Petrenko, Phys. Rev. Lett. **106**, 197204 (2011).
[6] G. Allodi, R. De Renzi, S. Agrestini, C. Mazzoli, and M. R. Lees, Phys. Rev. B **83**, 104408 (2011).
[7] C. L. Fleck, M. R. Lees, S. Agrestini, G. J. McIntyre, and O. A. Petrenko, Europhys. Lett. **90**, 67006 (2010).
[8] H. Fjellvag, E. Gulbrandsen, S. Aasland, A. Olsen, and B. C. Hauback, J. Solid State Chem. **124**, 190 (1996).
[9] Y. B. Kudasov, Europhys. Lett. **78**, 57005 (2007).
[10] L. C. Chapon, Phys. Rev. B **80**, 172405 (2009).
[11] R. Bindu, K. Maiti, S. Khalid, and E. V. Sampathkumaran, Phys. Rev. B **79**, 094103 (2009).
[12] J. Paddison, A. Agrestini, M. R. Lees, C. L. Fleck, P. P. Deen, A. L. Goodwin, J. R. Stewart, and O. A. Petrenko, arXiv:1312.5243 (2014).
[13] V. Hardy, S. Lambert, M. R. Lees, and D. McK. Paul, Phys. Rev. B **68**, 014424 (2003).
[14] S. Agrestini, L. C. Chapon, A. Daoud-Aladine, J. Schefer, A. Gukasov, C. Mazzoli, M. R. Lees, and O. A. Petrenko, Phys. Rev. Lett. **101**, 097207 (2008).
[15] H. Kageyama, K. Yoshimura, K. Kosuge, H. Mitamura, and T. Goto, J. Phys. Soc. Jpn. **66**, 1607 (1997).
[16] V. Hardy, D. Flahaut, R. Fresard, and A. Maignan, J. Phys.: Condens. Matter **19**, 145229 (2007).
[17] K. Adachi, K. Takeda, F. Matsubara, M. Mekata, and T. Haseda, J. Phys. Soc. Jpn. **52**, 2202 (1983).
[18] M. Mekata and K. Adachi, J. Phys. Soc. Jpn. **44**, 806 (1978).
[19] S. Agrestini, C. Mazzoli, A. Bombardi, and M. R. Lees, Phys. Rev. B **77**, 140403 (2008).
[20] Y. B. Kudasov, Phys. Rev. Lett. **96**, 027212 (2006).
[21] A. Maignan, V. Hardy, S. Hebert, M. Drillon, M. R. Lees, O. Petrenko, D. M. Paul, and D. Khomskii, J. Mater. Chem. **14**, 1231 (2004).
[22] R. Soto, G. Martinez, M. N. Baibich, J. M. Florez, and P. Vargas, Phys. Rev. B **79**, 184422 (2009).
[23] C. Mazzoli, A. Bombardi, S. Agrestini, and M. R. Lees, Physica B **404**, 3042 (2009).
[24] V. Hardy, M. R. Lees, O. A. Petrenko, D. McK. Paul, D. Flahaut, S. Hébert, and A. Maignan, Phys. Rev. B **70**, 064424 (2004).
[25] M. H. Qin, K. F. Wang, and J. M. Liu, Phys. Rev. B **79**, 172405 (2009).
[26] M. Zukovic, L. Mizisin, and A. Bobak, Phys. Lett. A **376**, 1731 (2012).
[27] A. Maignan, C. Michel, A. C. Masset, C. Martin, and B. Raveau, Eur. Phys. J. B **15**, 657 (2000).
[28] T. Goko, N. Nomura, S. Takeshita, and J. Arai, J. Magn. Magn. Mater. **272**, E633 (2004).
[29] S. Takeshita, T. Goko, J. Arai, and K. Nishiyama, J. Phys. Chem. Solids **68**, 2174 (2007).

[30] V. K. Pecharsky and K. A. Gschneidner, J. Appl. Phys. **86**, 565 (1999).
[31] M. H. Phan, V. Franco, A. Chaturvedi, S. Stefanoski, G. S. Nolas, and H. Srikanth, Phys. Rev. B **84**, 054436 (2011).
[32] M. H. Phan, M. B. Morales, N. S. Bingham, H. Srikanth, C. L. Zhang, and S. W. Cheong, Phys. Rev. B **81**, 094413 (2010).
[33] N. S. Bingham, P. Lampen, M. H. Phan, T. D. Hoang, H. D. Chinh, C. L. Zhang, S. W. Cheong, and H. Srikanth, Phys. Rev. B **86**, 064420 (2012).
[34] H. Aoki, T. Sakakibara, K. Matsuhira, and Z. Hiroi, J. Phys. Soc. Jpn. **73**, 2851 (2004).
[35] L. Q. Yan, S. H. Chun, Y. Sun, K. W. Shin, B. G. Jeon, S. P. Shen, and K. H. Kim, J. Phys.: Condens. Matter **25**, 256006 (2013).
[36] V. Hardy, D. Flahaut, M. R. Lees, and O. A. Petrenko, Phys. Rev. B **70**, 214439 (2004).
[37] J. A. Mydosh, *Spin Glasses: An Experimental Introduction*, (Taylor & Francis, London, 1993).
[38] J. L. Dormann, D. Fiorani, and E. Tronc, J. Magn. Magn. Mater. **202**, 251 (1999).
[39] S. Rayaprol, K. Sengupta, and E. V. Sampathkumaran, Phys. Rev. B **67**, 180404 (2003).
[40] E. V. Sampathkumaran and A. Niazi, Phys. Rev. B **65**, 180401 (2002).
[41] K. A. Gschneidner and V. K. Pecharsky, Mater. Sci. Engr. A **287**, 301 (2000).
[42] O. Tegus, E. Bruck, L. Zhang, Dagula, K. H. J. Buschow, and F. R. de Boer, Physica B **319**, 174 (2002).
[43] P. L. Paulose, N. Mohapatra, and E. V. Sampathkumaran, Phys. Rev. B **77**, 172403 (2008).
[44] A. Berton, J. Chaussy, J. Odin, R. Rammal, and R. Tournier, J. Physique Lett. **43**, L153 (1982).
[45] J. S. Amaral and V. S. Amaral, Appl. Phys. Lett. **94**, 042506 (2009).
[46] L. Caron, Z. Q. Ou, T. T. Nguyen, D. T. C. Thanh, O. Tegus, and E. Bruck, J. Magn. Magn. Mater. **321**, 3559 (2009).
[47] C. L. Fleck, *Magnetism in the Complex Cobaltates* $Y1-xSr_xCoO_3$ *(0.7* $\leq x \leq$ *0.95) and* $Ca_3Co_2O_6$. (The University of Warwick, Coventry, 2011).
[48] H. Kageyama, K. Yoshimura, K. Kosuge, X. Xu, and S. Kawano, J. Phys. Soc. Jpn. **67**, 357 (1998).
[49] O. A. Petrenko, J. Wooldridge, M. R. Lees, P. Manuel, and V. Hardy, Euro. Phys. J. B **47**, 79 (2005).
[50] S. M. Yusuf, A. Jain, and L. Keller, J. Phys. Condens. Matter **25**, 146001 (2013).